Dalton Transactions



PAPER



Cite this: *Dalton Trans.*, 2019, **48**, 13732

Received 6th August 2019, Accepted 27th August 2019 DOI: 10.1039/c9dt03199e

rsc.li/dalton

Solvent-responsive cavitand lanthanum complex†

Francesca Guagnini,^a Alessandro Pedrini, ^b Timothy M. Swager, ^b Chiara Massera*^a and Enrico Dalcanale *

Stimuli-responsive supramolecular assemblies are dynamic systems that can reversibly switch between different states upon external stimuli. In this context, metal coordination offers a reliable strategy for the preparation of stimuli responsive supramolecular architectures. Herein we report the preparation of a solvent-responsive cavitand-lanthanum coordination complex. A tetra-phosphonate cavitand has been functionalized with four hydroxyl moieties at the upper rim to form a pre-organized octadentate ligand capable of binding lanthanum salts. Exploiting the orthogonal recognition sites, two different complex architectures are formed in acetonitrile and acetone, respectively. The complexes have been characterized in solution by NMR spectroscopy, ITC experiments, while at the solid state, the single crystal structure of the acetonitrile derivative has been determined. Furthermore, as observed by DOSY-NMR spectroscopy, small quantities of acetone in acetonitrile are sufficient to trigger assembly interconversion.

Introduction

Metal coordination-directed self-assembly is a powerful tool to obtain sophisticated supramolecular architectures. ^{1–5} In this context, macrocyclic compounds, like calixarenes and cavitands with their unique shape and recognition properties, have been widely exploited as multidentate ligands. ^{6–16} The resulting coordination complexes have found application in many fields, including mimic biological systems, ^{12,17,18} catalysis, ^{19–21} molecular machines, ¹⁴ guest adsorption, ^{22,23} the development of metal organic frameworks ^{9,16,24–26} and tuning liquid-crystalline behaviour. ¹⁵

The design of systems that respond to an external stimulus is a major goal of supramolecular chemistry. ^{27–30} Indeed, stimuli-responsive supramolecular assemblies are pivotal in the design of smart materials. ^{8,31–33} Solvent often plays a key role in the nature of the resulting assembly, especially when it comes to metal coordination complexes. ^{30,34–37} The same building blocks (*i.e.* metal and organic ligand) can yield alternative structures when assembled in different solvents. ^{34–37} This behaviour is also observed for coordination

complexes of macrocyclic ligands. For example, methylene-bridged cavitand complexes with palladium behave as either bowls or capsules when assembled in water or chloroform/methanol solutions, respectively. Sometimes only small changes in solvent polarity are sufficient to promote assembly differentiation. Severin and co-workers reported a coordination cage that responds differently to two very similar solvents, namely chloroform and dichloromethane. Furthermore, coordinating solvents like acetonitrile, have been shown to induce racemization in resorcinarene-based capsules.

Herein we report a novel tetra-phosphonate cavitand-lanthanum complex that presents a solvent-dependent architecture both in solution and in the solid-state. Tetra-phosphonate cavitands are rigid bowl-shaped macrocycles constructed on a resorcinarene scaffold, featuring phosphonates as bridging groups. When all four P=O groups are pointing inward with respect to the cavity, ³⁹ the resulting rigid tetradentate receptor is able to coordinate only a limited number of metals, either directly or through second sphere coordination mediated by water. ⁴⁰ The formation of dimeric capsules with barium, calcium, zinc, ⁴⁰ lead and copper ⁴¹ has been demonstrated.

In this work, we functionalized the upper rim of a tetraphosphonate cavitand with four hydroxyl moieties, which can act as coordination sites for oxyphilic metals, such as lanthanides. This is promoted by the fact that hard Lewis acids, such as Ln³+ ions, have the tendency to prefer hard ligands, in particular oxygen donors. ⁴² Coordination of trivalent cations to tetra-phosphonate cavitands has not been yet investigated. Previous data suggested the radius of the cation dictates the coordination mode. ⁴¹ Hence, lanthanum was selected for this study as representative of the lanthanide series. The cavitand

^aDipartimento di Scienze Chimiche, della Vita e della Sostenibilità Ambientale and INSTM UdR Parma, Università di Parma, Parco Area delle Scienze 17/A, 43123 Parma (PR), Italy

^bDepartment of Chemistry and Institute for Soldier Nanotechnologies, Massachusetts Institute of Technology, 77 Massachusetts Avenue, Cambridge, Massachusetts 02139, USA

[†] Electronic supplementary information (ESI) available: NMR spectra, ITC titration experiments, crystallographic data, radius models. CCDC 1921340. For ESI and crystallographic data in CIF or other electronic format see DOI: 10.1039/c9dt03199e

ligand behaviour towards lanthanum was studied in acetonitrile, acetone and methanol. Our results show that the solvent dictates both the formation/dissociation of the complex and the architecture of the resulting assembly.

Materials and methods

Synthesis and product characterization

Unless stated otherwise, reactions were conducted in flamedried glassware under an atmosphere of argon using anhydrous solvents (either freshly distilled or passed through activated alumina columns). All commercially obtained reagents were used as received unless otherwise specified. Silica column chromatography was performed using silica gel 60 (Fluka 230-400 mesh or Merck 70-230 mesh). NMR spectra were obtained using a Bruker AVANCE 400 (400 MHz) spectrometer at 25 °C. 1 H and 13 C NMR chemical shifts (δ) were reported in ppm relative to the proton resonances resulting from incomplete deuteration of the NMR solvents. ³¹P NMR chemical shifts (δ) were reported in ppm relative to external 85% H₃PO₄. High resolution mass spectra were collected with a Bruker Daltonics APEXIV 4.7 Tesla Fourier Transform Ion Spectrometer (FT-ICR-MS) Cyclotron Resonance Mass equipped with an electrospray ionization sources (ESI). Resorcinarene I was synthesized according to a published procedure.43

Synthesis of resorcinarene [C₃H₇, CH₂OCH₂CH₂OAllyl](II)

To a suspension of resorcinarene I (0.5 g, 0.76 mmol) in 8 mL of acetonitrile, 2-allyloxyethanol (3.26 mL, 30.45 mmol) was added, followed by a 37% aqueous solution of formaldehyde (0.286 mL, 3.81 mmol). After the addition of iminodiacetic acid (0.051 g, 0.38 mmol), the mixture was refluxed for 16 h. After cooling, chloroform (100 mL) was added and the organics were separated and washed with water (3 \times 100 mL). The solvent was removed under reduced pressure and flash column chromatography (gradient from Hex/EtOAc 7:3 to Hex/EtOAc 1:1) afforded pure resorcinarene II as a white solid (0.283 g, 0.25 mmol, 33%).

¹H NMR (CDCl₃, 400 MHz): δ (ppm) = 8.58 (s, 8H, OH), 7.17 (s, 4H, ArH_{down}), 5.93 (m, 4H, OCH₂CH \rightleftharpoons CH₂), 5.26 (m, 8H, CH₂CH \rightleftharpoons CH₂), 4.82 (s, 8H, ArCH₂O), 4.33 (t, 4H, J = 7.9 Hz, CHCH₂), 4.03 (dt, 8H, J = 5.7 Hz, J = 1.4 Hz, OCH₂CH \rightleftharpoons CH₂), 3.69 (m, 8H, ArCH₂OCH₂CH₂O), 3.60 (m, 8H, ArCH₂OCH₂CH₂O), 2.28 (q, 8H, J = 7.4 Hz, CHCH₂CH₂), 1.30 (sext, 8H, J = 7.4 Hz, CH₂CH₂CH₃), 0.97 (t, 12H, J = 7.4 Hz, CH₂CH₃).

ESI-FT-ICR-MS: Calculated for $C_{64}H_{92}NO_{16} [M + NH_4]^+ m/z = 1130.642$, found m/z = 1130.642; calculated for $C_{64}H_{88}O_{16}Na [M + Na]^+ m/z = 1135.597$, found m/z = 1135.603.

Tetra-phosphonate cavitand [C₃H₇, CH₂OCH₂CH₂OAllyl, Et](III)

To a solution of resorcinarene II (0.170 g, 0.15 mmol) in 8 mL of pyridine, dichloroethylphosphine (70 μ L, 0.67 mmol) was added. The mixture was heated at 80 °C for 3 h. After cooling,

2 mL of aqueous 35% $\rm H_2O_2$ were added at 0 °C and the mixture was stirred for 1 h. The reaction was quenched with water (100 mL) and the precipitate was filtered, washed with water and dried. Cavitand III was obtained as a white solid (0.191 g, 0.14 mmol, 89%).

¹H NMR (CDCl₃, 400 MHz): δ (ppm) = 7.10 (s, 4H, ArH_{down}), 5.89 (m, 4H, OCH₂CH=CH₂), 5.22 (m, 8H, CH₂CH=CH₂), 4.73-4.58 (m, 12H, CHCH₂ + ArCH₂O), 3.99 (d, 8H, J = 5.7 Hz, OCH₂CH=CH₂), 3.65 (m, 8H, ArCH₂OCH₂CH₂O), 3.60 (m, 8H, ArCH₂OCH₂CH₂O), 2.20 (m, 16H, J = 7.4 Hz, P(O)CH₂CH₃ + CHCH₂CH₂), 1.51-1.28 (m, 20H, P(O)CH₂CH₃ + CH₂CH₂CH₃), 1.00 (t, 12H, J = 7.4 Hz, CH₂CH₃).

³¹**P NMR** (CDCl₃, 162 MHz): δ (ppm) = 22.3 (s, P=O).

ESI-FT-ICR-MS: Calculated for $C_{72}H_{104}NO_{20}P_4$ [M + NH₄]⁺ m/z = 1426.610, found m/z = 1426.609; calculated for $C_{72}H_{100}O_{20}P_4Na$ [M + Na]⁺ m/z = 1431.566, found m/z = 1431.571.

Tetra-phosphonate cavitand [C₃H₇, CH₂OCH₂CH₂OH, Et] (1)

Cavitand III (0.378 g, 0.27 mmol) was dissolved in 20 mL of a degassed mixture of $CH_2Cl_2/MeOH$ (1:3), followed by the addition of $Pd(PPh_3)_4$ (0.031 g, 0.027 mmol). 1,3-Dimethylbarbituric acid (0.335 g, 2.15 mmol) was added and the reaction mixture was stirred at room temperature for 18 h. The solvent was removed under reduced pressure and the crude was recrystallized from toluene twice affording pure cavitand 1 as yellowish solid (0.188 g, 0.15 mmol, 56%).

¹H NMR (CD₃OD, 400 MHz): δ (ppm) = 7.55 (s, 4H, ArH_{down}), 4.74 (t, 4H, J = 7.9 Hz, CHCH₂), 4.59 (s, 8H, ArCH₂O), 3.66 (m, 8H, ArCH₂OCH₂CH₂OH), 3.55 (m, 8H, ArCH₂OCH₂CH₂OH), 2.47–2.29 (m, 16H, J = 7.4 Hz, P(O) CH₂CH₃ + CHCH₂CH₂), 1.55–1.34 (m, 20H, P(O)CH₂CH₃ + CH₂CH₃), 1.08 (t, 12H, J = 7.4 Hz, CH₂CH₃).

³¹**P NMR** (CD₃OD, 162 MHz): δ (ppm) = 25.8 (s, P=O).

¹³C NMR (CD₃OD, 100 MHz): δ (ppm) = 145.7, 135.0, 123.9, 123.4, 71.9, 63.1, 60.8, 36.3, 32.7, 29.4, 20.7, 18.4, 17.5, 12.8, 5.4.

ESI-FT-ICR-MS: $m/z = 1266.55 [M + NH₄]^+$.

NMR samples

NMR samples were prepared by dissolving cavitand 1 and an equimolar amount of $LaCl_3$ in acetonitrile- d_3 or acetone- d_6 . 1% of water was added to favour dissolution. 5% of acetone was also added in the case of the assembly interconversion experiment.

DOSY-NMR

DOSY-NMR spectra were acquired at 20 °C on a 600 MHz JEOL spectrometer. The spectra were acquired with a bbp_dste_led sequence with gradient spoiling, using 32 scans. The gradient strength was logarithmic incremented of 16 steps from 0 to 0.55 T m⁻¹. Diffusion time was set to 0.1 s, delta was 1.2 ms and the relaxation delay was 7 s. Diffusion coefficient values were obtained by fitting peak intensity decays in Delta 5.3.0 software using the curve analysis option.

Paper Dalton Transactions

ITC experiments

Titrations were performed in acetonitrile or acetone at 25 °C on a MicroCal PEAQ-ITC System. To reach complete dissolution of the two components, 5% water was added to both solvents. The ITC titrations were performed by adding incremental amounts of cavitand 1 to the LaCl₃ solution placed in the cell of the calorimeter. Stoichiometry and thermodynamic parameters were calculated as the average of three experiments. The heat released upon binding was tracked against time (Fig. S7 and S8,† top trace). To account for unspecific heats of dilution, 1 was also titrated into pure solvent (blank titration). In all cases, the signal from blank titrations was subtracted from the binding signal before curve fitting with single-site model (Fig. S7 and S8,† bottom trace).

X-Ray crystallography

The solid-state structures of La-1 and 1 were determined by X-ray diffraction methods on single crystals. Crystal data and experimental details for data collection and structure refinement are reported in Table S1.† Intensity data and cell parameters were recorded at 190(2) K on a Bruker D8 Venture PhotonII diffractometer equipped with a CCD area detector, using a MoK α radiation (λ = 0.71073 Å).

The raw frame data were processed using SAINT and SADABS to yield the reflection data file. A4,45 The structures were solved by Direct Methods using the SIR97 program and refined on F_o^2 by full-matrix least-squares procedures, using SHELXL-2014 in the WinGX suite v.2014.1. In the case of La-1, all non-hydrogen atoms were refined with anisotropic atomic displacements, except when disorder was present. The hydrogen atoms were included in the refinement at idealized geometry (C-H 0.95-0.99 Å, O-H 0.82 Å) and refined "riding" on the corresponding parent atoms with $U_{\rm iso}(H)$ set to $1.2U_{\rm eq}(C)$ and $1.5U_{\rm eq}(O, C_{\rm met})$. When possible, the H atoms of the water molecules were found in the difference Fourier map. The weighting scheme used in the last cycle of refinement was $w = 1/[\sigma^2 F_o^2 + (0.0662P)^2 + 4.1299P]$, where $P = (F_o^2 + 2F_c^2)/3$.

Crystallographic data for La-1 have been deposited with the Cambridge Crystallographic Data Centre as supplementary publication no. CCDC 1921340. \dagger

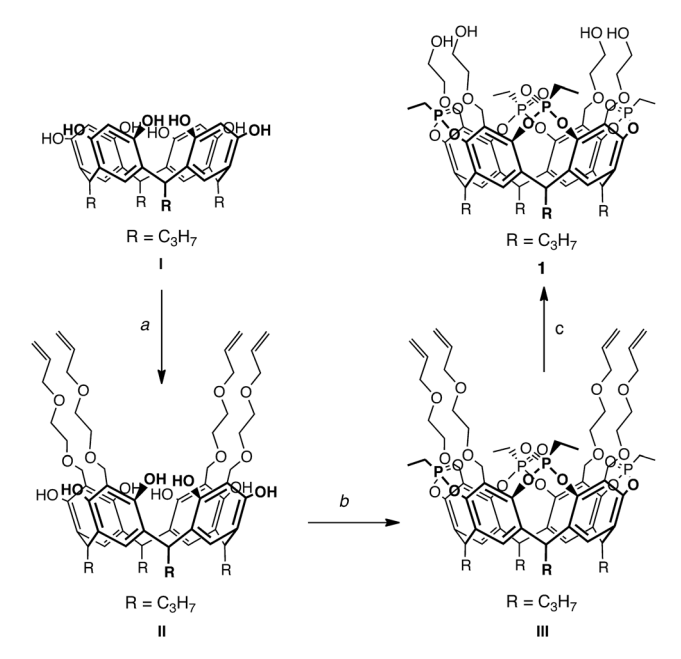
Crystals of 1 diffracted poorly, and the data were not good enough to refine its structure. However, it was possible to determine the species which was formed and its bond connectivity. See the ESI† for its main crystallographic data.

Results and discussion

Synthesis of cavitand 1

Cavitand 1, bearing four hydroxyl groups at the upper rim, was synthesized in three steps from resorcinarene I with 16% overall yield (Scheme 1). The Mannich reaction with the alcohols is a straightforward strategy for the functionalization of resorcinarene apical positions.⁴⁹

The iminodiacetic acid-catalysed reaction of ${\bf I}$ with 2-allyloxy-ethanol and formaldehyde afforded resorcinarene ${\bf II}$ with four



Scheme 1 Synthesis of cavitand 1. (a) 2-Allyloxyethanol, CH_2O aq. 37%, iminodiacetic acid, acetonitrile, 84 °C, 12 h, 33%; (b) (1) $EtPCl_2$, pyridine, 80 °C, 3 h; (2) H_2O_2 35%, r.t., 1 h, 89% (over two steps); (c) $Pd(PPh_3)_4$, 1,3-dimethylbarbituric acid, $CH_2Cl_2/MeOH$, r.t., 12 h, 56%.

allyl-protected hydroxyl groups in apical position. Protection of the aliphatic alcohol allowed for subsequent bridging of the resorcinarene phenols with dichloroethylphosphine, followed by *in situ* oxidization with hydrogen peroxide affording tetraphosphonate cavitand **III**. Pd-catalysed deprotection, using 1,3-dimethylbarbituric acid as an allyl scavenger, gave tetrahydroxyl cavitand **1**.

Solution state characterization

Lanthanum complexes were assembled by mixing equimolar amounts of cavitand 1 and LaCl₃ in acetonitrile or acetone.

¹H and ³¹P 1D-NMR spectra were measured in both solvents and the signals were compared with those of the free ligand (Fig. 1 and 2). In both cases, the chemical shift perturbation confirmed the formation of the complex. Glycol signals (H4 and H5) in the proton NMR spectra (Fig. 1) are shifted downfield, suggesting lanthanum coordination at this site.

Notably, methylene H3 connecting the aromatic scaffold to the upper rim chain is shifted upfield in acetonitrile (Fig. 1, left) and downfield in acetone (Fig. 1, right). This difference suggests a non-innocent role played by the solvent in the complex assembly.

It has been demonstrated that, depending on the dimensions of the cationic radius involved, phosphonate groups are challenged to behave as direct ligands for the metal centres, and in many cases more likely form H-bonds with the water molecules of the metal aquo complexes, thus participating as a second coordination sphere. To investigate the involvement of the P=O moieties in the formation of the complex, the TP NMR spectra were analysed. A shift of the phosphonate groups

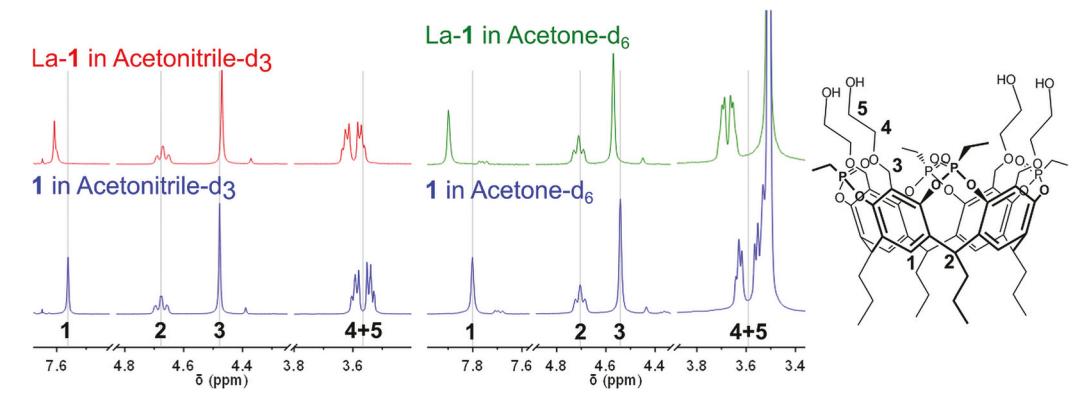


Fig. 1 Portions of the ¹H NMR spectra of cavitand 1 (bottom) and its lanthanum complexes (top) in acetonitrile-d₃ (left) and acetone-d₆ (right). The panels highlight signals of protons 1 to 5 assigned as shown in the molecule diagram. Vertical grey lines are added to guide the reader.

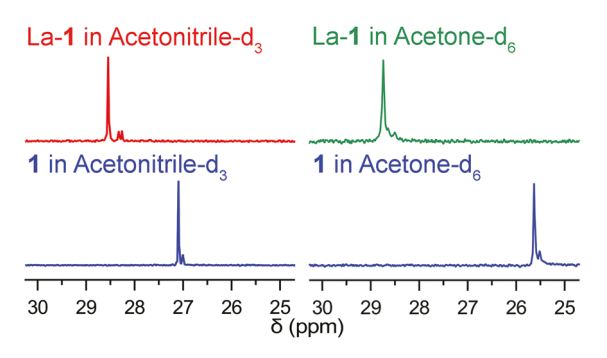


Fig. 2 Comparison between the ^{31}P NMR spectra of cavitand 1 (bottom) and La-1 complex (top) in acetonitrile-d₃ (left) and acetone-d₆ (right).

upon addition of the lanthanum salt was clearly observed (Fig. 2). The P=O signal is shifted of ≈ 1.5 ppm in acetonitrile and of ≈ 3 ppm in acetone, likely as a result of a second sphere coordination of the P=Os to La³⁺. At a first glance, this observation could point to the formation of stronger interactions between the lanthanum ion and cavitand 1 in acetone. However, a careful observation reveals that the different chemical shift perturbations rely in the initial chemical shifts of the phosphonate groups of cavitand 1 in the two solvents.

Moreover, the encapsulation of guests in the cavity of tetra-phosphonate cavitands strongly depends on C-H··· π interactions. The methyl group of acetonitrile is electron-poor and can interact with the electron-rich cavity, as confirmed by crystallographic data. The encapsulation of acetonitrile in the cavity gives rise to signals at upfield chemical

shifts for ligand 1, reducing the chemical shift perturbation from the complex formation. On the other hand, acetone is not a suitable guest for the cavity, but behaves as crystallization solvent, as observed for previously reported structures.⁵³

Isothermal Titration Calorimetry (ITC) studies were performed to further investigate the nature of the complexes in solution. The ITC experiments allowed the assessment of both stoichiometry and thermodynamic signature of the complexation process in acetonitrile and acetone. In the two tested solvents, a 1:1 stoichiometry of the complexation was evidenced from the inflection point in the titration curves plotted as heat νs . molar ratio of cavitand to metal ion (Fig. S7 and S8†). Moreover, a single-site (monovalent) theoretical model was found to properly fit all the experimental binding curves, leading to the determination of the thermodynamic parameters ΔH , K_a , ΔG , and $T\Delta S$, which are summarized in Table 1.

In the two solvents, the complexation of La³⁺ with cavitand 1 is an endothermic reaction, dominated by entropy. Such unfavourable enthalpic contribution is common for the complexation of metal cations in aqueous solutions, since the pairing event requires the extended desolvation of both metal cation and cavitand binding site.^{54,55} This assumption is not always applicable to complexations in organic solvents, especially when weakly coordinating solvents are involved.^{56,57} The following parameters should be considered for the evaluation of solvent ability to donate electron pairs to a metal ion: donor number (DN), donor strength (DS) and coordination power (CP)⁵⁸ The DN, DS, and CP values of water (18, 17, 0.79), which is present in considerable percentage in the organic solutions, are much larger than those of acetonitrile (14.1, 12, 0) and acetone (17, 15, -0.48). For this reason, it is correct to con-

Table 1 Thermodynamic parameters obtained from ITC experiments for the complexation of La³⁺ with cavitand 1 in acetonitrile and acetone

| Solvent | n | $K_{a}\left(\mathbf{M}^{-1}\right)$ | $\Delta H (kJ \text{ mol}^{-1})$ | ΔG (kJ mol ⁻¹) | $T\Delta S$ (kJ mol ⁻¹) |
|---------------------------|--------------|-------------------------------------|----------------------------------|------------------------------------|-------------------------------------|
| Acetonitrile ^a | 0.86 (±0.04) | $2.36 (\pm 0.09) \times 10^5$ | $36.0 (\pm 0.8)$ | -30.61 (±0.02) | 66.8 (±0.9) |
| Acetone ^a | 0.97 (±0.06) | $1.74 (\pm 0.16) \times 10^4$ | $9.9 (\pm 0.7)$ | -24.2 (±0.2) | 34.1 (±0.9) |

^a 5% water is added to reach LaCl₃ dissolution.

Paper Dalton Transactions

sider that the solvation core around La³⁺, as well as that of the cavitand upper rim, is dominated by water molecules.

Crystallography

X-ray diffraction analysis gave further insights on the complex formed in acetonitrile. Plate-like, colourless crystals were obtained by slow evaporation of a solution of La-1 in acetonitrile + 1% water, revealing the formation of a 1:1 ligand: metal complex of general formula $[(1)La(CH_3CN)(H_2O)_7]$ $Cl_3\cdot 3CH_3CN\cdot 3H_2O$ (Fig. 3).

In the complex, the four upper-rim chains of the cavitand are all stretched out in the plane perpendicular to the aromatic scaffold and only one hydroxyl group is coordinated to lanthanum through its oxygen atom O5A. The coordination sphere around the metal is completed by the nitrogen atom N1S of one acetonitrile molecule and by the seven water molecules O1W–O7W (selected bond lengths are reported in Table S2†). The three chloride counterions Cl1–Cl3 are located in the lattice, stabilized by a network of H-bonds with the free (O8W–O10W) and coordinated water molecules, and with the OH groups of the hydroxyl chains (see Table S3†).

As can be seen in Fig. 4, the solvent plays a crucial role in the supramolecular structure of the complex and is responsible for the formation of a dimer. The acetonitrile molecule coordinated by lanthanum via the free electron pair on the CN is at the same time encapsulated in the cavity of a symmetry-related cavitand through C-H··· π interactions [C2S-H2SB···Cg1: 3.813(3) Å and 156.2(8)°; C2S-H2SC···Cg2: 3.880(4) Å and 127.0(8)°. Cg1 and Cg2 are the centroids of the aromatic rings C1B-C6B and C1C-C6C, respectively].

Furthermore, two of the water molecules coordinated by lanthanum form H-bonds directly with the P=O groups of the symmetry-related cavitand $[O4W-H7W\cdots O3D^i: 2.713(4) \text{ Å}$ and $171(2)^\circ$; $O7W-H13W\cdots O3A^i: 2.729(5) \text{ Å}$ and $165(4)^\circ$. i=1-x, -y, 1-z]. The formation of such a second-sphere coordination complex between the tetraphosphonate cavitand **1** and the lanthanum acquo-cation was to be expected on the basis of previously reported results with $Zn(\pi)^{40}$ and $Cu(\pi)^{41}$ Here, the

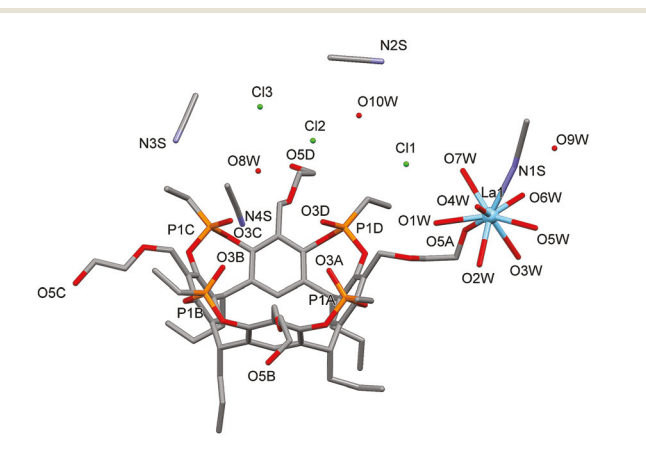


Fig. 3 Asymmetric unit of $[(1)La(CH_3CN)(H_2O)_7]Cl_3\cdot 3CH_3CN\cdot 3H_2O$ with partial labelling scheme. H atoms and disordered alkyl chains have been omitted for clarity.

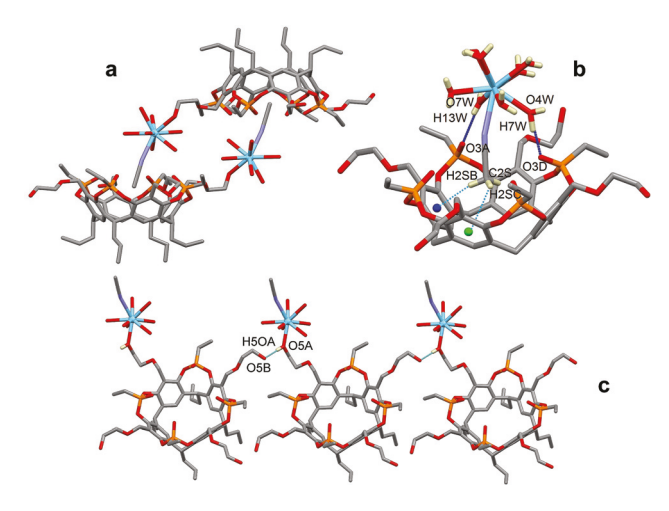


Fig. 4 (a) View of the solvent-mediated supramolecular dimer formed by La-1. Lattice solvent molecules, H atoms and chloride anions have been omitted for clarity. The symmetry code to generate half of the dimer is 1-x, -y, 1-z. (b) View of the relevant weak interactions (blue and cyan dotted lines) forming the supramolecular dimer in La-1. Cg1 and Cg2 are shown as blue and green spheres, respectively. (c) The H-bonded chain formed by La-1 along the b-axis direction.

concomitant presence of acetonitrile and of flexible hydroxyl chains appears to trigger dimerization over the formation of a dimeric capsule.

DOSY-NMR spectroscopy

The possibility to form dimeric species also in solution was investigated by Diffusion Ordered Spectroscopy (DOSY) NMR. DOSY-NMR is a valid technique for the estimation of the diffusion coefficient value (D) for supramolecular assemblies in solution.^{59,60} Assuming that the species volume in solution is spherical, D relates to the hydrodynamic radius (r) through the Stokes–Einstein equation ($D = k_{\rm b}T/6\pi\eta r$). For non-spherical species, shape and size corrections need to be applied yielding $D = k_{\rm b}T/c\pi\eta r f_{\rm h}$, where $f_{\rm h}$ is the shape factor and c the size factor.

Nevertheless, for supramolecular molecules and capsules the Stokes-Einstein equation remains a valid approximation.⁵⁹ The value of r accounts for the whole solvation sphere of the species, namely for coordinated solvent molecules. For this reason, the hydrodynamic radius of the pristine ligand was measured in both solvents and used as a comparison (Table 2).

While ITC highlighted a 1:1 stoichiometry in both solvents, DOSY-NMR showed a remarkable difference in hydrodynamic radius. In acetonitrile, the radius of the complex ($\approx 13 \text{ Å}$) was double than that determined for the ligand alone ($\approx 7 \text{ Å}$), which is consistent with the formation of a dimeric species (Fig. S11 and S12†). This observation matches the solid-state data, confirming the presence of the dimeric assembly in solution. Most likely, ITC experiments in acetonitrile did not provide evidence for two separated coordination and dimerization events since they happen simultaneously. It is likely that the interplay among lanthanum coordination to the

Table 2 Diffusion coefficient and hydrodynamic radius for cavitand 1 and its lanthanum complex in acetonitrile and acetone

| | Diffusion coefficient (m ² s ⁻¹) | Hydrodynamic radius ^a (Å) |
|------------------------|---|---|
| 1 in acetonitrile | $7.7 (\pm 0.13) \times 10^{-10}$ | 7 |
| La-1 in acetonitrile | $4.0 (\pm 0.06) \times 10^{-10}$ | 13 |
| 1 in acetone | $8.2 (\pm 0.12) \times 10^{-10}$ | 8 |
| La-1 in acetone | $6.1 (\pm 0.09) \times 10^{-10}$ | 10 |
| La-1 in acetonitrile + | $5.8 (\pm 0.10) \times 10^{-10}$ | $\approx 9^b$ |
| 10% acetone | ` ' | |

 a r is calculated based on the Stokes–Einstein equation. See the main text and the experimental section for details. b An approximate value for r is reported, as η was considered equal to acetonitrile viscosity for the calculation.

hydroxyl groups, the second sphere coordination of the P=O to coordinated water molecules and the encapsulation of acetonitrile drive the formation of the dimer. Acetone is not a suitable guest for tetra-phosphonate cavitands and cannot be encapsulated by the cavity. Hence, the complex in acetone is expected to be a discrete monomeric species. Comparison between the hydrodynamic radius (Table 2) of the complex and the ligand corroborated this hypothesis. The ligand radius (\approx 8 Å) is comparable with the radius of the complex (\approx 10 Å). The difference is most likely a result of the presence of lanthanum.

To probe the solvent responsiveness in solution, a small quantity of acetone (10%) was added to the acetonitrile solution of complex La-1 and the D coefficient was measured via DOSY-NMR (Table 2). Remarkably, the small addition of acetone was enough to trigger the assembly interconversion; indeed, the hydrodynamic radius decreased to a value of ca. 9 Å, suggesting the formation of a monomeric species. 1D spectra acquired after the addition, showed broadening of the peaks of the glycol protons, indicative of a phenomenon happening at this site (Fig. S13†).

Proposed mechanism

To understand this mechanism two factors must be taken into account: (i) the preference of La^{3+} for acetone or acetonitrile as a ligand and (ii) the affinity of the two solvents for the cavity of

tetra-phosphonate cavitands. Lanthanides are generally considered hard metals and are therefore often defined as oxyphilic. 42,61

Furthermore, acetone is known to complete the coordination sphere of La³⁺ when used as a solvent. 62-64 Also acetonitrile coordination to La³⁺ has been reported multiple times. 65-69 Nevertheless, acetonitrile is not tightly bound and can be exploited as a labile ligand in lanthanide complex synthesis. 69,70 It is plausible to conclude that, when acetone is added to La-1 in acetonitrile, the solvent molecules compete for La³⁺ coordination, thereby displacing acetonitrile from the coordination sphere. Coordinated acetone molecules, however, are poor guests for the cavity and cannot displace the encapsulated acetonitrile. This mechanism breaks the dimer apart and prompts the La-1 architecture interconversion. The proposed mechanism for architecture interconversion of La-1 is report in Fig. 5.

Once formed, the complex can be fully dis-assembled in a protic solvent like methanol. When exposed to methanol, the La-1 crystals dissolved and recrystallized, to yield cavitand 1 in a solvated form. The diffraction data were not of high enough quality to perform a full refinement of the structure, nevertheless, the cavitand and the solvent molecules could be uniquely identified (Fig. S10†). The asymmetric unit comprises half a molecule of 1 and two half molecules of methanol. One methanol is held inside the cavity by H-bonding with the P=O groups and participates in C-H \cdots π interactions with the aromatic walls. The second methanol molecule is H-bonded to the methanol inside the cavity but does not interact directly with the macrocycle. The crystal structure is probably stabilized by weak H-bonding interactions involving the OH groups of the upper rim chains, which are all stretched out in the plane perpendicular to the aromatic scaffold similarly to what observed in the lanthanum complex.

Conclusions

The solvent-responsive behaviour of a tetra-phosphonate cavitand-lanthanum complex has been elucidated. An *ad-hoc* functionalized tetra-phosphonate cavitand 1 was synthetized dec-



Fig. 5 Cartoon of the proposed mechanism for the assembly and interconversion of La-1. Cavitand 1 (left) forms a dimeric complex with lanthanum (yellow sphere), stabilised by encapsulation of two acetonitrile molecules (blue rods). The complex is held together by H-bonding between the P=O moieties and an aquo-lanthanum core. Acetone (red) substitutes acetonitrile in the coordination sphere of La³⁺ and triggers interconversion of the complex into a monomeric species. See the main text for details.

Paper Dalton Transactions

orating the apical positions with four hydroxyl moieties. La³⁺ coordinates 1 in solutions of acetonitrile and acetone as indicated by NMR characterization. In addition to thermodynamic data assessed by ITC, DOSY-NMR spectroscopy suggests a dimeric assembly for the complex in acetonitrile and a monomeric assembly in acetone. In the case of acetonitrile, the solvent-driven dimeric assembly was also proved to be present in the solid-state. Interconversion from the dimeric species to the monomeric species was achieved by addition of acetone to an acetonitrile solution of La-1 complex. Furthermore, preliminary crystallography data suggested full disassembly of the complex in a protic solvent like methanol.

We have proposed a model wherein two variables play a crucial role in selecting the complex architecture: (i) the coordinating ability of the solvent and (ii) the encapsulation of the solvent in the cavity of a tetra-phosphonate cavitand. Such solvent-responsive behaviour has not been observed previously for tetra-phosphonate cavitand-metal complexes. The newly synthesized La-1 complex represents a further steppingstone in the design of stimuli-responsive supramolecular architectures based on macrocyclic ligands.

Conflicts of interest

There are no conflicts to declare.

Acknowledgements

This research was supported by a grant to TMS from the NSF DMR-1809740 and University of Parma intramural funding (PhD fellowship to FG). This work has also benefited from the equipment and framework of the COMP-HUB Initiative, funded by the 'Departments of Excellence' program of the Italian Ministry for Education). D. Acquotti and S. Ghelli are thanked for assistance with NMR spectroscopy. Chiesi Farmaceutici SpA is acknowledged for the support with the D8 Venture X-ray equipment.

Notes and references

- 1 D. Tian, Q. Chen, Y. Li, Y.-H. Zhang, Z. Chang and X.-H. Bu, *Angew. Chem., Int. Ed.*, 2014, 53, 837–841.
- 2 M. Han, D. M. Engelhard and G. H. Clever, *Chem. Soc. Rev.*, 2014, 43, 1848–1860.
- 3 T. R. Cook and P. J. Stang, *Chem. Rev.*, 2015, **115**, 7001–7045.
- 4 H. Zhang, R. Zou and Y. Zhao, *Coord. Chem. Rev.*, 2015, 292, 74–90.
- 5 S. Zarra, D. M. Wood, D. A. Roberts and J. R. Nitschke, *Chem. Soc. Rev.*, 2015, **44**, 419–432.
- 6 N. Cuminetti, M. H. K. Ebbing, P. Prados, J. De Mendoza and E. Dalcanale, *Tetrahedron Lett.*, 2001, **42**, 527–530.
- 7 T. Haino, K. Fukuta, H. Iwamoto and S. Iwata, *Chem. Eur. J.*, 2009, 15, 13286–13290.

8 L. Shao, J. Yang and B. Hua, *Polym. Chem.*, 2018, **9**, 1293–1297.

- 9 S. P. Bew, A. D. Burrows, T. Düren, M. F. Mahon, P. Z. Moghadam, V. M. Sebestyen and S. Thurston, *Chem. Commun.*, 2012, 48, 4824–4826.
- 10 T. Chavagnan, D. Sèmeril, D. Matt, J. Harrowfield and L. Toupet, *Chem. Eur. J.*, 2015, **21**, 6678–6681.
- 11 F. L. Thorp-Greenwood, T. K. Ronson and M. J. Hardie, *Chem. Sci.*, 2015, **6**, 5779–5792.
- 12 J.-N. Rebilly, B. Colasson, O. Bistri, D. Over and O. Reinaud, *Chem. Soc. Rev.*, 2015, **44**, 467–489.
- 13 R. Pinalli, E. Dalcanale, F. Ugozzoli and C. Massera, *CrystEngComm*, 2016, 18, 5788–5802.
- 14 M. Nakamura, K. Kishimoto, Y. Kobori, T. Abe, K. Yoza and K. Kobayashi, *J. Am. Chem. Soc.*, 2016, **138**, 12564–12577.
- 15 G. Yu, Y. Ye, Z. Tong, J. Yang, Z. Li, B. Hua, L. Shao and S. Li, *Macromol. Rapid Commun.*, 2016, 37, 1540–1547.
- 16 M. Moradi, L. G. Tulli, J. Nowakowski, M. Baljozovic, T. A. Jung and P. Shahgaldian, *Angew. Chem., Int. Ed.*, 2017, 56, 14395–14399.
- 17 S. Rat, J. Gout, O. Bistri and O. Reinaud, *Org. Biomol. Chem.*, 2015, 13, 3194–3197.
- 18 G. De Leener, D. Over, C. Smet, D. Cornut, A. G. Porras-Gutierrez, I. López, B. Douziech, N. Le Poul, F. Topić, K. Rissanen, Y. Le Mest, I. Jabin and O. Reinaud, *Inorg. Chem.*, 2017, 56, 10971–10983.
- 19 D. Vidal, M. Costas and A. Lledó, ACS Catal., 2018, 8, 3667–3672.
- 20 J. Hong, K. E. Djernes, I. Lee, R. J. Hooley and F. Zaera, ACS Catal., 2013, 3, 2154–2157.
- 21 N. Natarajan, E. Brenner, D. Sémeril, D. Matt and J. Harrowfield, *Eur. J. Org. Chem.*, 2017, **2017**, 6100–6113.
- 22 W.-Y. Pei, G. Xu, J. Yang, H. Wu, B. Chen, W. Zhou and J.-F. Ma, *J. Am. Chem. Soc.*, 2017, **139**, 7648–7656.
- 23 Q.-Y. Zhai, J. Su, T.-T. Guo, J. Yang, J.-F. Ma and J.-S. Chen, *Cryst. Growth Des.*, 2018, **18**, 6046–6053.
- 24 M. Schulz, A. Gehl, J. Schlenkrich, H. A. Schulze, S. Zimmermann and A. Schaate, *Angew. Chem., Int. Ed.*, 2018, 57, 12961–12965.
- 25 Y. B. Dong, H. Y. Shi, J. Yang, Y. Y. Liu and J. F. Ma, *Cryst. Growth Des.*, 2015, **15**, 1546–1551.
- 26 B.-B. Lu, J. Yang, Y.-Y. Liu and J.-F. Ma, *Inorg. Chem.*, 2017, 56, 11710–11720.
- 27 M. Nakahata, Y. Takashima, H. Yamaguchi and A. Harada, *Nat. Commun.*, 2011, 2, 511.
- 28 S. Dong, J. Yuan and F. Huang, Chem. Sci., 2014, 5, 247-252.
- 29 M. Zhang, X. Yan, F. Huang, Z. Niu and H. W. Gibson, Acc. Chem. Res., 2014, 47, 1995–2005.
- 30 A. J. Mcconnell, C. S. Wood, P. P. Neelakandan and J. R. Nitschke, *Chem. Rev.*, 2015, **115**, 7729–7793.
- 31 X. Yan, F. Wang, B. Zheng and F. Huang, *Chem. Soc. Rev.*, 2012, 41, 6042.
- 32 M. Xue, Y. Yang, X. Chi, X. Yan and F. Huang, *Chem. Rev.*, 2015, 115, 7398–7501.
- 33 J. Mendez-Arroyo, A. I. d'Aquino, A. B. Chinen, Y. D. Manraj and C. A. Mirkin, *J. Am. Chem. Soc.*, 2017, 139, 1368–1371.

34 K. Suzuki, M. Kawano and M. Fujita, *Angew. Chem., Int. Ed.*, 2007, **46**, 2819–2822.

- 35 O. Mamula, M. Lama, H. Stoeckli-Evans and S. Shova, *Angew. Chem., Int. Ed.*, 2006, **45**, 4940–4944.
- 36 S. J. Park, D. M. Shin, S. Sakamoto, K. Yamaguchi, Y. K. Chung, M. S. Lah and J.-I. Hong, *Chem. Eur. J.*, 2005, **11**, 235–241.
- 37 B. Kilbas, S. Mirtschin, R. Scopelliti and K. Severin, *Chem. Sci.*, 2012, 3, 701–704.
- 38 T. Imamura, T. Maehara, R. Sekiya and T. Haino, *Chem. Eur. J.*, 2016, 22, 3250–3254.
- 39 R. Pinalli, M. Suman and E. Dalcanale, *Eur. J. Org. Chem.*, 2004, **2004**, 451–462.
- 40 M. Melegari, C. Massera, F. Ugozzoli and E. Dalcanale, *CrystEngComm*, 2010, **12**, 2057–2059.
- 41 R. Pinalli, E. Dalcanale, K. Misztal, R. Lucentini, F. Ugozzoli and C. Massera, *Inorg. Chim. Acta*, 2018, **470**, 250–253.
- 42 C.-H. H. Huang, Rare Earth Coordination Chemistry: Fundamentals and Applications, Wiley-VCH, 2010.
- 43 L. M. Tunstad, J. A. Tucker, E. Dalcanale, J. Weiser, J. A. Bryant, J. C. Sherman, R. C. Helgeson, C. B. Knobler and D. J. Cram, *J. Org. Chem.*, 1989, 54, 1305–1312.
- 44 SADABS Bruker AXS, 2004.
- 45 SAINT Software Users Guide Version 6.0 Bruker Analytical X-ray Systems, 1999.
- 46 A. Altomare, M. C. Burla, M. Camalli, G. L. Cascarano, C. Giacovazzo, A. Guagliardi, A. G. G. Moliterni, G. Polidori and R. Spagna, *J. Appl. Crystallogr.*, 1999, 32, 115–119.
- 47 G. M. Sheldrick, *Acta Crystallogr.*, *Sect. A: Found. Crystallogr.*, 2008, **64**, 112–122.
- 48 L. J. Farrugia, J. Appl. Crystallogr., 1999, 32, 837-838.
- 49 M. Urbaniak and W. Iwanek, *Tetrahedron*, 2006, **62**, 1508–1511.
- 50 M. Dionisio, G. Oliviero, D. Menozzi, S. Federici, R. M. Yebeutchou, F. P. Schmidtchen, E. Dalcanale and P. Bergese, J. Am. Chem. Soc., 2012, 134, 2392–2398.
- 51 E. Biavardi, G. Battistini, M. Montalti, R. M. Yebeutchou, L. Prodi and E. Dalcanale, *Chem. Commun.*, 2008, **14**, 1638–1640.

- 52 M. Melegari, C. Massera, R. Pinalli, R. M. Yebeutchou and E. Dalcanale, *Sens. Actuators, B*, 2013, **179**, 74–80.
- 53 C. Massera, M. Melegari, E. Kalenius, F. Ugozzoli and E. Dalcanale, *Chem. Eur. J.*, 2011, 17, 3064–3068.
- 54 C. Bonal, Y. Israëli, J.-P. Morel and N. Morel-Desrosiers, *J. Chem. Soc., Perkin Trans.* 2, 2001, 7, 1075–1078.
- 55 G. H. Nancollas, Coord. Chem. Rev., 1970, 5, 379-415.
- 56 A. F. Danil de Namor and O. Jafou, J. Phys. Chem. B, 2001, 105, 8018–8027.
- 57 K. Kano, M. Kondo, H. Inoue, H. Kitagishi, B. Colasson and O. Reinaud, *Inorg. Chem.*, 2011, **50**, 6353–6360.
- 58 M. Sandström, I. Persson, P. Persson, E. K. Euranto, T. Brekke, D. W. Aksnes and T. Tokii, *Acta Chem. Scand.*, 1990, 44, 653–675.
- 59 L. Avram and Y. Cohen, Chem. Soc. Rev., 2015, 44, 586-602.
- 60 A. Macchioni, G. Ciancaleoni, C. Zuccaccia and D. Zuccaccia, *Chem. Soc. Rev.*, 2008, 37, 479–489.
- 61 R. H. Crabtree, *The Organometallic Chemistry of the Transition Metals*, Wiley-VCH, 2014.
- 62 E. Terazzi, S. Torelli, G. Bernardinelli, J.-P. Rivera, J.-M. Bénech, C. Bourgogne, C. Donnio, D. Guillon, D. Imbert, J.-C. G. Bünzli, A. Pinto, D. Jeannerat and D. Piguet, J. Am. Chem. Soc., 2005, 127, 888–903.
- 63 K. Gholivand, H. Mostaanzadeh, T. Koval, M. Dusek, M. F. Erben, H. Stoeckli-Evans and C. O. Della Védova, *Acta Crystallogr., Sect. B: Struct. Sci.*, 2010, 66, 441–450.
- 64 L. K. Macreadie, H. E. Maynard-Casely, S. R. Batten, D. R. Turner and A. S. R. Chesman, *ChemPlusChem*, 2015, 80, 107–118.
- 65 M. N. Bochkarev, G. V. Khoroshenkov, H. Schumann and S. Dechert, *J. Am. Chem. Soc.*, 2003, **125**, 2894–2895.
- 66 K. Gholivand, H. R. Mahzouni, M. Pourayoubi and S. Amiri, *Inorg. Chim. Acta*, 2010, 363, 2318–2324.
- 67 M. J. D. Champion, P. Farina, W. Levason and G. Reid, *Dalton Trans.*, 2013, **42**, 13179.
- 68 J. F. Corbey, D. H. Woen, J. W. Ziller and W. J. Evans, *Polyhedron*, 2015, **103**, 44–50.
- 69 P. N. Hazin, J. W. Bruno and G. K. Schulte, *Organometallics*, 1990, **9**, 416–423.
- 70 J. L. Brown, B. L. Davis, B. L. Scott and A. J. Gaunt, *Inorg. Chem.*, 2015, 54, 11958–11968.